

Supporting Information for
“Improving Robustness of Fifth-Rung Functionals with Linearized Ladder Correlation”

Ella R. Ransford and Kevin Carter-Fenk*

Department of Chemistry, University of Pittsburgh, Pittsburgh, Pennsylvania 15218, USA

(Dated: May 8, 2026)

*kay.carter-fenk@pitt.edu

1. Additional Computational Details

1.1. Transition Metal Bond Dissociation Energies In order to compare with experimental results for bond dissociation energies (BDEs), we accounted for zero-point vibrational energies at the equilibrium geometry including the harmonic term ω_e and the first anharmonic correction $\omega_e x_e$ which were both obtained from Ref. 1. We also use the computed spin-orbit coupling corrections from Ref. 1 to account for spin-orbit effects in the following way,

$$\Delta E_{\text{SOC}} = E_{\text{SOC}}^A + E_{\text{SOC}}^B - E_{\text{SOC}}^{AB} \quad (\text{S1})$$

where A and B are individual atoms in the transition-metal diatomic. The total corrected dissociation energy that is compared with experiment is,

$$D_e = D_0 + \frac{1}{2}\omega_e - \frac{1}{4}\omega_e x_e + \Delta E_{\text{SOC}} \quad (\text{S2})$$

where

$$D_0 = E^A + E^B - E^{AB} \quad (\text{S3})$$

is the dissociation energy computed for a given functional at 0 K. All calculations employed an X2C Hamiltonian to account for scalar relativistic effects. For the $\omega\text{B97M}(2)$ functional, the X2C corrections needed to be added in *post hoc* by computing $\Delta\text{X2C} = \text{BDE}(\text{X2C}) - \text{BDE}(\text{non-rel})$ with the similar $\omega\text{B97M-V}$ functional and adding ΔX2C to the computed BDE of $\omega\text{B97M}(2)$. Finally, errors are computed as the distance to the nearest (upper or lower) error delimiter of the benchmark experimental data.

All BDEs for this data set were computed using the Def2-QZVPPD basis set. The sensitivity to basis set was assessed briefly on this set of transition metal diatomic BDEs by contrasting mean absolute errors obtained with Def2-ma-TZVPP and Def2-QZVPPD basis sets. Our results in Table S1 show that $\omega\text{B97M}(2)$ retains an astonishing consistency between basis sets with just a 0.1 kcal/mol change in mean absolute deviation. We find that $\omega\text{B97X-L-V}$ is less sensitive than most functionals tested, and appears to be similarly sensitive as $\omega\text{B97X-2-D3}$ to improvements in the basis set beyond the Def2-ma-TZVPP basis in which it was parameterized.

Finally, while only a simple example, we found that increasing the basis set quality on the A24 set of noncovalent interactions had no effect on the MAE, which was 0.1 kcal/mol in each case. However, for S22 there is a somewhat greater effect, with the MAE improving from 0.3 kcal/mol to 0.2 kcal/mol upon improving the quality of the basis set. This finding certainly motivates the development of more efficient algorithms for LinLCCD(hh) correlation so that larger basis sets may be more routinely employed.

Table S1. Change in mean absolute error (ΔMAE) from Def2-ma-TZVPP \rightarrow Def2-QZVPPD basis sets for 3d transition-metal diatomic bond dissociation energies. All results in kcal/mol

Functional	ΔMAE
$\omega\text{B97M}(2)$	0.1
$\omega\text{B97X-L-V}$	0.6
$\omega\text{B97X-2-D3}$	0.6
$\omega\text{DSD72-PBEP86-D4}$	1.2
B2GGPLYP-D3	1.4
B2NC-PLYP-D3	2.1
Pr ² SCAN69-D4	2.2

1.2. Asymptotic Estimates of Bond Dissociation Energies with Restricted Orbitals In the main text, we reported the BDEs of 19 species computed with restricted orbitals via $E(r = 10,000 \text{ \AA}) - E(r_{\text{eq}}) = E_{\text{BDE}}$. For singlet O_2 and B_2 , we computed the BDEs at the CCSDTQ level using an aug-cc-pVDZ/aug-cc-pVTZ two-point extrapolation to the complete basis set (CBS) limit,

$$E_{\text{corr}}^{\text{CBS}} = \frac{X^3 E_{\text{corr}}^{aTZ} - Y^3 E_{\text{corr}}^{aDZ}}{X^3 - Y^3} \quad (\text{S4})$$

where $X = 3$ and $Y = 2$ correspond to basis set cardinality. The core 1s orbitals were frozen in these calculations. The CBS limit mean-field contribution was estimated by computing the Hartree-Fock SCF energy at the aug-cc-pV5Z level, such that

$$E_{\text{CBS}} \approx E_{\text{HF}}^{a5Z} + E_{\text{corr}}^{\text{CBS}} \quad (\text{S5})$$

To test the accuracy of this procedure, we applied it to C_2 , for which there are high-accuracy/high-precision experimental data available. After back-correcting the experimental result as shown above with ω_e , $\omega_e x_e$, and spin-orbit corrections, we find that our CCSDTQ/CBS estimate of the BDE is within 2% of experiment. Other than the two excited state molecules (singlet B_2 and O_2), we refer to back-corrected experimental data (using Eq. S2) for the systems that do not appear in the W4-11 data base. All corrected experimental data use spectroscopic parameters available on NIST². If unavailable on NIST, any other zero-point vibrational corrections used are specifically cited within the main text.

2. Potential Energy Curves

The torsional profile of ethylene featured in Fig. S2 was generated via constrained optimizations at 5° increments at the CASSCF(12,12)/cc-pVDZ level of theory. Higher-quality CASSCF(12,12)/cc-pVTZ calculations were carried out at each point, and these serve as the benchmark for the shape of the torsional profile. Unrestricted orbitals were used for all DFT calculations, and internal stability was assessed at each point to guarantee the lowest energy solution was found.

The π and π^* orbitals of ethylene become degenerate at the $\theta = 90^\circ$ geometry, leading to strong correlation. Despite this, the largest errors relative to CASSCF(12,12)/cc-pVTZ appear in the intermediate twist geometries between 50° - 65° . The maximum errors along the potential surface are summarized as ω DSD72-PBEP86-D4 > Pr²SCAN69-D4 \sim ω B97X-2-D3 > ω B97X-L-V > ω B97M(2), suggesting that ω B97X-L-V performs reasonably well. Similarly, the errors in the torsional barrier height are summarized as Pr²SCAN69-D4 > ω B97X-2-D3 \sim ω B97X-L-V > ω DSD72-PBEP86-D4 > ω B97M(2). Overall, the errors across the torsional profile as assessed by the average of the maximum error and the magnitude of the barrier height error are summarized as Pr²SCAN69-D4 > ω DSD72-PBEP86-D4 > ω B97X-2-D3 > ω B97X-L-V > ω B97M(2). Like the transition metal diatomic BDE results presented in the main text, these results suggest that ω B97X-L-V performs similarly to other top performing functionals in the description of strongly correlated systems.

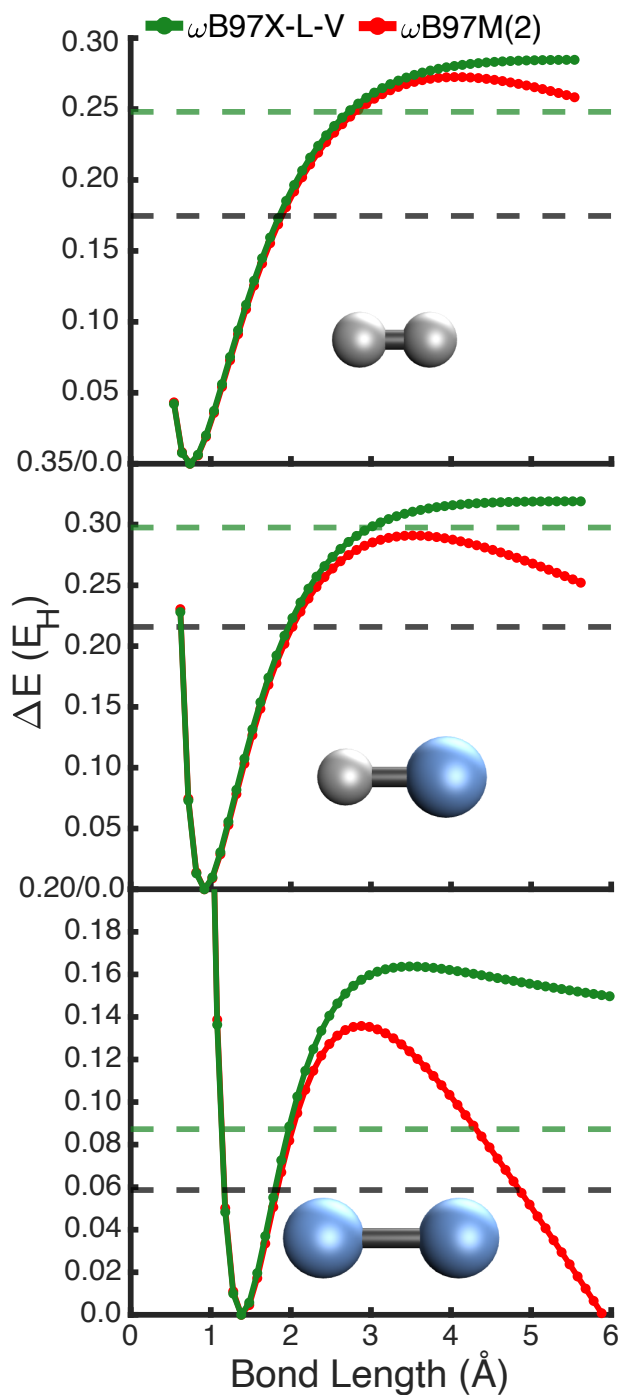


Figure S1. Restricted Kohn-Sham bond dissociation potential energy surfaces for H_2 (top panel), HF (middle panel), and F_2 (bottom panel) using $\omega\text{B97X-L-V}$ and $\omega\text{B97M(2)}$ functionals in the Def2-ma-TZVPP basis set. Green dashed lines show the asymptotic dissociation limit (estimated at a bond length of 10,000 Å) for $\omega\text{B97X-L-V}$, and the gray dashed line shows the benchmark dissociation energy. No finite dissociation limit can be provided for $\omega\text{B97M(2)}$ as the MP2 correlation energy diverges at large distances.

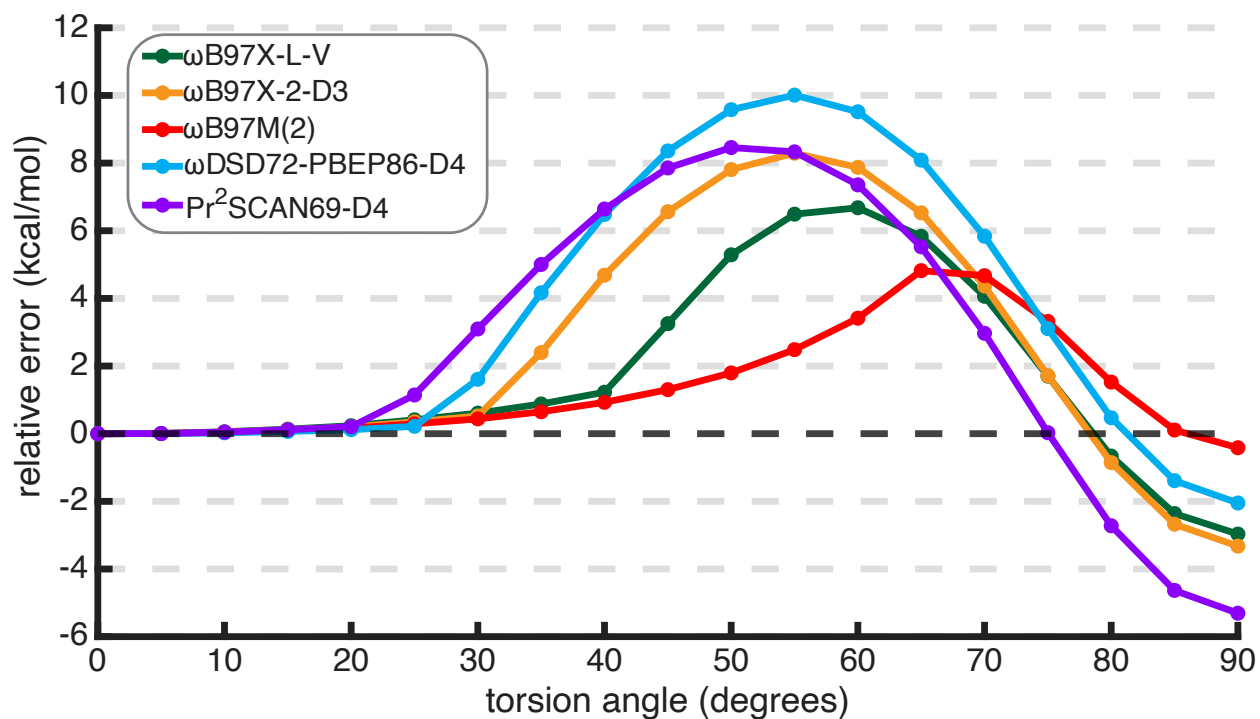


Figure S2. Relative errors in the topography of the torsional profile of ethylene about the C=C bond, computed using unrestricted orbitals in the Def2-ma-TZVPP basis set. All curves are shifted such that the energy at the planar geometry (0°) is zero. The relative energies are calculated with respect to the CASSCF(12,12)/cc-pVTZ potential surface.

-
- ¹ Y. A. Aoto, A. P. d. Batista, A. Köhn and A. G. S. de Oliveira-Filho, *J. Chem. Theory Comput.*, 2017, **13**, 5291–5316.
- ² R. D. Johnson, *NIST Computational Chemistry Comparison and Benchmark Database, NIST Standard Reference Database Number 101*, 2022.